Electronic Supplementary Material (ESI) for Chemical Communications

Light-activated ruthenium complexes photobind DNA and are cytotoxic in the photodynamic therapy window

Erin Wachter, David K. Heidary, Brock S. Howerton, Sean Parkin, and Edith C. Glazer

Supplementary Information

1. General Procedures.

Materials: All chemicals were obtained from commercial sources and were used without further purification.

Instruments: All ^{1}H NMR were obtained on a Varian Mercury spectrometer (400 MHz) and chemical shifts reported relative to the residual solvent peak of acetonitrile at δ 1.94 or methanol at δ 3.31. The ^{13}C chemical shifts are reported relative to CD_3CN at δ 1.39. Electrospray ionization (ESI) mass spectra were obtained on a Varian 1200L mass spectrometer at the University of Kentucky Environmental Research Training Laboratory (ERTL). Absorption spectra were obtained on an Agilent 8453 Diode Array spectrophotometer. Photoexpulsion experiments were performed using a Dell 200 Watt 1410X projector (for *in vitro* photoejection experiments) or 410 Watt 955

Model 900 AJH projector (for cell cytotoxicity studies). The more intense light source was used for the cell cytotoxicity studies in order to minimize the time the samples would be removed from the incubation chamber in order to reduce cell death due to temperature and atmosphere alterations. Edmund Optics filters (item numbers NT43-941, NF49-935, NT43-947, and NT43-954) were used to cut off the appropriate sections of the UV and visible spectrum. UV/Vis experiments were performed in a 1-cm pathlength quartz cuvette placed 12 inches from the projector. Kinetics were fit using the equation for a single exponential with the Prism software package. Cell survival was quantified using a Tecan SpectraFluor Plus Microplate Reader.

Photoejection kinetics:

The ruthenium compounds were added to 3 mL of dH_2O in a quartz cuvette for a final concentration between 30-80 μM. The sample was placed in a small box protected from ambient light covered with the appropriate filter, and then irradiated with light from a Dell 1410X projector/200 W light source. Scans were taken after set time points to monitor the process of ligand ejection until no change was observed. For compound **2** the IR filter was also used. The normalized change in absorbance was plotted to determine the half-life of ejection using Prism software.

HPLC analysis of purity and ejected ligand:

Ruthenium complexes and ligands were analyzed with an Agilent 1100 Series HPLC equipped with a model G1311A quaternary pump, G1315B UV diode array detector and Chemstation software version B.01.03. Chromatographic conditions were optimized on a Column Technologies Inc. C18 120 Å column (250 mm x 4.6 mm inner diameter, 5 μm) fitted with a Phenomenex C18 (4 mm x 3 mm) guard column. The detection wavelength was 280 nm. Mobile phases of 0.1 % formic acid in dH_2O and 0.1 % formic acid in HPLC grade acetonitrile were used in all studies.

Sample preparation:

The ruthenium complexes were dissolved in acetonitrile and placed into two vials. One vial was used to test the purity of the complex, and the second vial of each complex was activated under white light for 3 hours prior to injection on the HPLC. 2,2'-biquinoline and 1,10-Phenanthroline were dissolved in DMSO and diluted 10 fold into acetonitrile before injection to give a final concentration of 1 mg/mL.

Gradient Used:

Time (minutes)	0.1 % formic in dH_2O	0.1 % formic in MeCN
0	98	2
2	95	5
5	70	30
15	70	30
20	40	60
30	5	95
35	98	2
40	98	2

2. Synthesis.

The synthesis and purification of the compounds was performed under low ambient light in order to avoid photo-decomposition.

The synthesis of $[Ru(phen)_2Cl_2]$ was performed as described in the literature.[1] Briefly, $RuCl_3\ 3H_2O$ (1.00 g, 3.84 mmol), 1,10-phenanthroline monohydrate (1.895 g, 9.57 mmol), and LiCl (2.43 g, 57.36 mmol) were added to 100 mL of DMF in a round bottom flask. The mixture was refluxed for 23 hours, allowed to cool and dried down. Solid was dissolved in minimal DMF, precipitated with acetone, filtered and washed with acetone. The precipitate was dissolved in hot DMF, re-precipitated with acetone, filtered, and washed with acetone. Yield: 1.253 g (61.4%). $Ru(phen)_2(H_2O)_2$ was synthesized as previously reported.[2]

Compound 1 $[Ru(phen)_2biq]$: $Ru(phen)_2Cl_2$ (0.412 g, 0.774 mmol) and 2,2'-biquinoline (0.305 g, 1.19 mmol) were added to 8 mL degassed ethylene glycol in a pressure tube. The mixture was heated at 160 ^oC in the dark for 22.5 hours. The sample was allowed to cool to room temperature and poured into 50 mL of distilled water. Addition of a saturated KPF_6 solution produced a red precipitate that was collected by vacuum filtration. The red precipitate was washed with distilled water. Purification by precipitation as the Cl^- salt gave the pure complex. Yield: 722.4 mg (92.6%). ^1H NMR (CD_3OD, 400 MHz): δ 8.87 (d, *J* = 8.6 Hz, 2H), 8.71 (dd, *J* = 8.6, 1.2 Hz, 2H), 8.65 (d, *J* = 8.6 Hz, 2H), 8.58 (dd, *J* = 8.6, 1.2 Hz, 2H), 8.32 (dd, *J* = 5.5, 1.2 Hz, 2H), 8.25 (d, *J* = 9.0 Hz, 2H), 8.19 (d, *J* = 8.6 Hz, 2H), 7.95-7.90 (m, 4H), 7.83 (d, *J* = 5.1 Hz, 1H), 7.81 (d, *J* = 5.1 Hz, 1H), 7.56 (d, *J* = 5.5, 1H), 7.54 (d, *J* = 5.5 Hz, 1H), 7.41 (td, 8.2, 1.2 Hz, 2H), 7.04 (d, 9.0 Hz, 2H), 6.98-6.94 (m, 2H); ^{13}C NMR (CD_3CN, 100 MHz): δ 161.98, 155.70, 154.10, 152.18, 149.27, 148.56, 140.39, 138.51, 138.30, 132.37, 132.15, 132.02, 130.59, 130.13, 130.00, 129.28, 129.15, 127.22, 126.90, 125.75, 122.10, 21C; ESI MS calcd for $C_{42}H_{28}N_6Ru$ $[M]^+$ 718.14, $[M]^{2+}$ 359.07; found 718.3 $[M]^+$, 359.2 $[M]^{2+}$. UV/Vis (CH_3CN): λ_{max} nm (ε $M^{-1}cm^{-1}$) 218 (78,000), 338 (28,400), 378 (19,300), 440 (8,300), 525 (8,300).

The synthesis of $[Ru(biq)_2Cl_2]$ was performed as described in the literature.[1] Briefly, $RuCl_3\ 3H_2O$ (0.514 g, 1.966 mmol), 2,2'-biquinoline (0.993 g, 3.879 mmol), LiCl (1.218 g, 28.74 mmol), and ascorbic acid (0.245 g, 1.392 mmol) were added to 12.5 mL of anhydrous DMF in a round bottom flask. The mixture was refluxed under N_2 gas for 23 hours, allowed to cool and precipitated in acetone with diethyl ether at -20 ^oC for 2 hours. The mixture was filtered and washed with cold water, followed by diethyl ether. The green solid that was collected was dissolved into hot anhydrous DMF, re-precipitated in acetone with diethyl ether at -20 ^oC for 2 hours. The solid was filtered and washed with water and diethyl ether. Yield: 705 mg (52.3%).

Compound 2 $[Ru(biq)_2phen]$: $Ru(biq)_2Cl_2$ (0.105 g, 0.153 mmol) and 1,10-phenantholine monohydrate (0.034 g, 0.170 mmol) were added to 5 mL degassed ethylene glycol in a pressure tube. The mixture was heated at 160 ^oC in the dark for 6 hours, allowed to cool and transferred into 50 mL of distilled water. Addition of a saturated KPF_6 solution produced a purple precipitate that was collected by vacuum filtration. The purple solid was washed with distilled water, followed by diethyl ether. The purification of the solid was carried out by flash chromatography on SiO_2. Elution with $KNO_3/H_2O/MeCN$ (0.3/7/93) gave the pure complex. After column purification, the NO_3^- salt of the complex was dissolved in water with minimal acetonitrile. A saturated solution of KPF_6 was added to precipitate the complex. The PF_6^- salt of the complex was isolated by extraction into

methylene chloride, dried with $MgSO_4$, filtered, and the solvent removed under reduced pressure. Yield: 102.3 mg (61.5%). ^{1}H NMR (CD_3CN, 400 MHz): δ 9.10 (d, J = 8.8 Hz, 2H), 9.02 (d, J = 8.8 Hz, 2H), 8.84 (d, J = 9 Hz, 2H), 8.40 (d, J = 8.8 Hz, 2H), 8.32-8.29 (m, 4H), 8.18 (dd, J = 8.2, 1.1 Hz, 2H), 7.80 (2d, J = 8.2, 8.2 Hz, 2H), 7.70-7.67 (m, 4H), 7.53 (t, J = 7.5 Hz, 2H), 7.41 (d, J = 9 Hz, 2H), 7.24 (t, J = 7.5 Hz, 2H), 7.12-7.08 (m, 4H). 6.83 (t, J = 8.5 Hz, 2H); ^{13}C NMR (CD_3CN, 100 MHz): δ 161.35, 160.50, 152.70, 151.81, 150.23, 146.64, 140.26, 138.68, 137.79, 132.73, 130.44, 129.37, 129.52, 129.37, 129.23, 128.89, 128.75, 128.05, 127.44, 125.83, 125.39, 124.94, 122.50, 121.45, 24C; ESI MS calcd for $C_{48}H_{32}N_6Ru$ $[M]^+PF_6^-$ 939.14, $[M]^{2+}$ 397.09; found 939.1 $[M]^+$ PF_6^-, 397.0 $[M]^{2+}$. UV/Vis (CH_3CN): λ_{max} nm (ε $M^{-1}cm^{-1}$) 217 (38,100), 317 (19,600), 361 (16,400), 381 (17,800), 479 (3,600), 550 (5,000).

Counter Ion Exchange:

All compounds were converted to the chloride salt for biological testing. The complex as the PF_6^- salt was dissolved in a minimal volume of acetone (1-2 mL), followed by the addition of a solution of t-butyl ammonium chloride (1 g dissolved in 5 mL of acetone) to produce a precipitate. The precipitate was filtered through a cotton plug, washed with acetone, and eluted with acetonitrile. The solvent was removed under reduced pressure to give the pure product.

3. Biological Studies.

Measurement of energy output by light sources

The 200 W and 410 W projectors were measured for the power output generated by the lamp, using a 1918-R meter (Newport Corporation) in the presence of cutoff filters. For cell cytotoxicity measurements with blue, green, and red filters, the compounds were activated with 7 J/cm^2 of light (14 J/cm^2 of red light for the 6 minute time point). 40 J/cm^2 and 120 J/cm^2 of light was used for the *in vitro* activity assays for 1 and 3 hours, respectively. For studies with the near-IR filter, 42 J/cm^2 was used for the cell studies (5 J/cm^2 in 3 min of near-IR light) and 7 J/cm^2 was used for the *in vitro* 1 hour time point and 21 J/cm^2 for the 3 hour time point.

DNA Dosing and Light Activation:

Ru (II) complexes were serially diluted 1:2 to give final concentrations of 0, 15, 30, 60, 125, 250, 500 μM, and 1000 μM of compound with 40 μg/ml of pUC19 plasmid in 10 mM phosphate buffer pH 7.4. Dark control samples were removed prior to exposure of the plasmid-compound solution to light. The samples were then placed 12 inches from the 200 W lamp fitted with either blue, green, red or near-IR cut-off filters. After one and three hour(s) of irradiation, aliquots were removed and stored in the dark overnight. DNA loading dye was added to the samples prior to electrophoresis.

DNA control samples:

Control samples were generated to discriminate between single strand and double strand breaks in the compound-plasmid reactions. To induce single strand breaks, 40 μg/ml of pUC19 in 10 mM phosphate buffer, pH 7.4, was mixed with 8 μM $Cu(OP)_2$ (copper phenanthroline) and the reaction initiated upon the addition of DTT and H_2O_2 resulting in a final concentration of 1 mM for both reagents. The solution was mixed by vortexing for 10 seconds and the reaction was allowed to proceed at room temperature for 30 minutes. To induce double strand breaks in pUC19 the restriction enzyme, EcoRI, was used according to the manufacturer's instructions, using 40 μg/ml of plasmid. The reaction was allowed to proceed for 90 min at 37 ^{o}C, and then stored at -20 ^{o}C.

Gel Electrophoresis:
Samples with pUC19 plasmid were resolved on a 1% agarose gel in Tris-Acetate (TA) buffer, with 0.3 μg of plasmid loaded per lane. The samples were run for 75 min at 100 mV followed by staining the gel with a solution of 500 ng/ml Ethidium Bromide in TA buffer for 40 min. The gels were then destained in TA buffer for 30 min and digitally imaged with the FOTO/Analyst® Investigator equipped with the FOTO/Analyst® PC Image software, Version 10.41.

DNA Isolation:

Due to the apparent disappearance of the DNA at higher compound concentrations, as indicated by the significantly reduced EtBr signal (>98% at 250 μM, quantified using ImageJ) a DNA isolation experiment was performed. Samples were resolved on the agarose gel as described above, followed by excision of the bands and purification of the plasmid from the agarose with a gel extraction kit (Qiagen). Excision of the bands and the gel wells for the 0, 62, and 250 μM samples for gels shown in Fig. S6 A), B) and C) was performed. The samples were then measured for DNA content by following the optical density at 260 nm with a Nanodrop ND1000 microsample spectrophotometer. The sensitivity of the assay allowed for qualitative assessment of the DNA content, and showed that ca. 80% of the DNA was observed in the gel bands excised from the gel in the region of 2000 to 4000 bp even at the highest compound concentrations for gels A), B), and C). Minimal DNA was found in the wells. These results indicate that the disappearance of the majority of the EtBr fluorescence signal is due to a modification in the DNA structure, reducing EtBr binding, or by some inner filter effect with absorption of the EtBr emission by the Ru complexes. We cannot rule out the possibility of ca. 20% of the DNA being degraded.

Cell Biology:

Cell survival assay: The HL60 promyelocytic leukemia cell line was obtained from ATCC and maintained in IMDM media (Invitrogen) supplemented with 10% serum supreme (Lonza) and penicillin/streptomycin at 37 ^{o}C with 5% CO_2. For cytotoxicity assays, the cells were plated in Optimem supplemented with 1% serum supreme and penicillin/streptomycin at 30,000 cells per well in Costar 96 well flat bottom clear tissue culture treated plates. The compounds were dosed from 0 to 300 μM, incubated with the cells for 12 hours, and then light activated for the indicated times using a 410 W projector fitted with the appropriate cut-off filters at a distance of 12 inches from the lamp to the plate. The cells were then incubated for 72 hours followed by the addition of Cell Titer Glo (Promega) to determine viability. Dark controls were run in parallel. The resulting luminescence was measured with a SpectraFluor Plus Plate Reader (Tecan). Data were fit to the equation for a sigmoidal dose response using Prism Software. Experiments to determine the cytotoxicity of exposure to light alone were performed using blue, green, and red filters. Approximately 8% loss in cell viability was observed using the blue or green filters with 3 minutes of light exposure; no cell viability loss was observed using the red filter.

4. Crystallography.

The compounds were known to be unstable with respect to light. As a precaution, all crystal manipulations requiring exposure to light were conducted as rapidly as possible. To this end, the crystal(s) were plunged directly into liquid nitrogen and mounted using cryo-tongs[3] initially developed for crystals of biological macromolecules.

Single crystals of Compound 1 were grown from methylene chloride, mounted in inert oil and transferred to the cold gas stream of the diffractometer. X-ray diffraction data were collected at 90.0(2) K on a Bruker-Nonius X8 Proteum diffractometer with graded-multilayer focused CuK(alpha) x-rays. Raw data were integrated, scaled, merged and corrected for Lorentz-polarization effects using the APEX2 package.[4] Corrections for absorption were applied using either SADABS or TWINABS,[5] and by XABS2.[6] The structure was solved by direct methods (SHELXS-97[6]) and difference Fourier (SHELXL-97[7]). Refinement was carried out against F^2 by weighted full-matrix least-squares (SHELXL-97[7]), and assessed with the aid of an R-tensor.[8] Hydrogen atoms were found in difference maps but subsequently placed at calculated positions and refined using a riding model. Non-hydrogen atoms were refined with anisotropic displacement parameters. Atomic scattering factors were taken from the International Tables for Crystallography.[9] Crystal data and relevant details of the structure determinations are summarized below and selected geometrical parameters are given in Table S3.

Crystal data: $C_{87}H_{62}C_{16}F_{24}N_{12}P_4Ru_2$, M = 2270.21, monoclinic, a = 21.8129(4), b = 18.8565(4), c = 22.0760(4) Å, U = 8708.3(3) Å^3, T = 90.0(2) K, space group P21/c, Z = 4, 118686 reflections measured, 15730 unique (R_{int} = 0.0561). The final R1=0.0449 (I>2σ(I)).

Single crystals of Compound **2** were crystallized from acetone, mounted in inert oil and transferred to the cold gas stream of the diffractometer. X-ray diffraction data were collected at 90.0(2) K on a Nonius kappaCCD diffractometer using MoK(alpha) x-rays. Raw data were integrated, scaled, merged and corrected for Lorentz-polarization effects using the HKL-SMN package.[10] Corrections for absorption were applied using either SCALEPACK,[10] or SADABS,[5] and by XABS2.[6] The structure was solved by direct methods (SHELXS-97[7]) and difference Fourier (SHELXL-97[7]). Refinement was carried out against F^2 by weighted full-matrix least-squares (SHELXL-97[7]), with the aid of an R-tensor.[8] Hydrogen atoms were found in difference maps but subsequently placed at calculated positions and refined using a riding model. Non-hydrogen atoms were refined with anisotropic displacement parameters. Atomic scattering factors were taken from the International Tables for Crystallography.[9] Crystal data and relevant details of the structure determinations are summarized below and selected geometrical parameters are given in Table S2.

Crystal data: $C_{51}H_{38}F_{12}N_6OP_2Ru$, M = 1141.88, monoclinic, a = 12.5876(1), b = 15.9629(1), c = 23.7620(2) Å, U = 4681.82(6) Å^3, T = 90.0(2) K, space group P 21/n, Z = 4, 103415 reflections measured, 10763 unique (R_{int} = 0.0699). The final R1=0.0474 (I>2σ(I)).

5. Additional Figures.

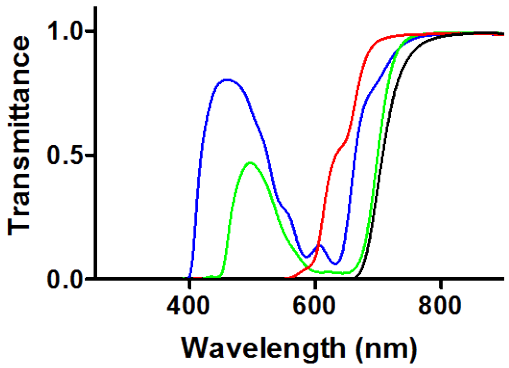

Figure S1. Plot of transmittance of Edmond Optics filters used in all light activated experiments. Blue: blue filter; green: green filter; red: red filter; black: near-IR cutoff filter.

	Compound 1	**Compound 2**
$t_{1/2}$ Blue (>400 nm)	8.7 min	53 sec
$t_{1/2}$ Green (>450 nm)	24.8 min	1.8 min
$t_{1/2}$ Red (>600 nm)	122.6 min	10.7 min
$t_{1/2}$ Near IR (>650 nm)	N/A	2.6 hr

Table S1. Half-life of ligand ejection with different wavelengths of light in dH_2O.

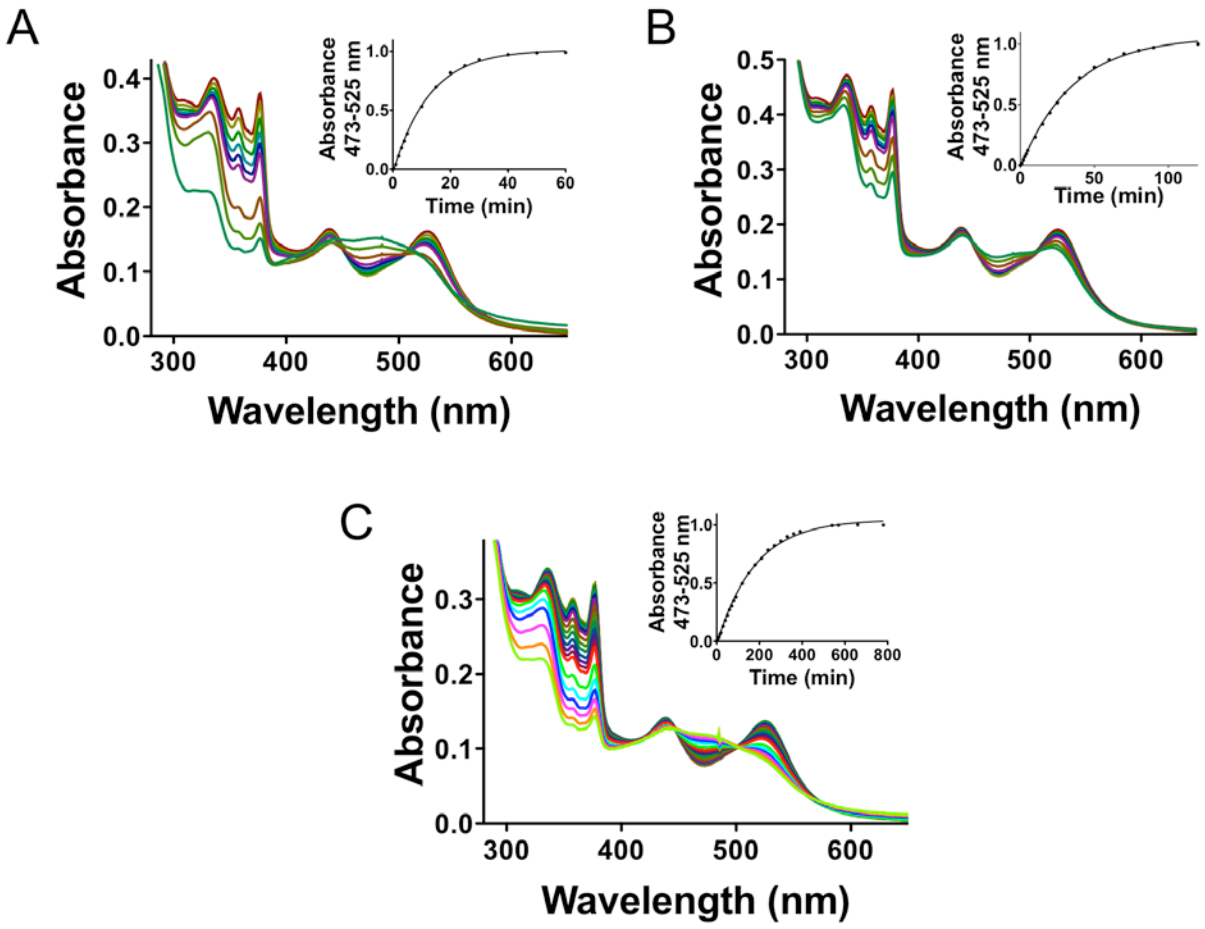

Figure S2. Plots of photoejection kinetics of compound **1** in dH_2O followed by UV-Vis. The kinetic fit is shown in the inset. A) photoejection with blue filter; B) photoejection with green filter; C) photoejection with red filter.

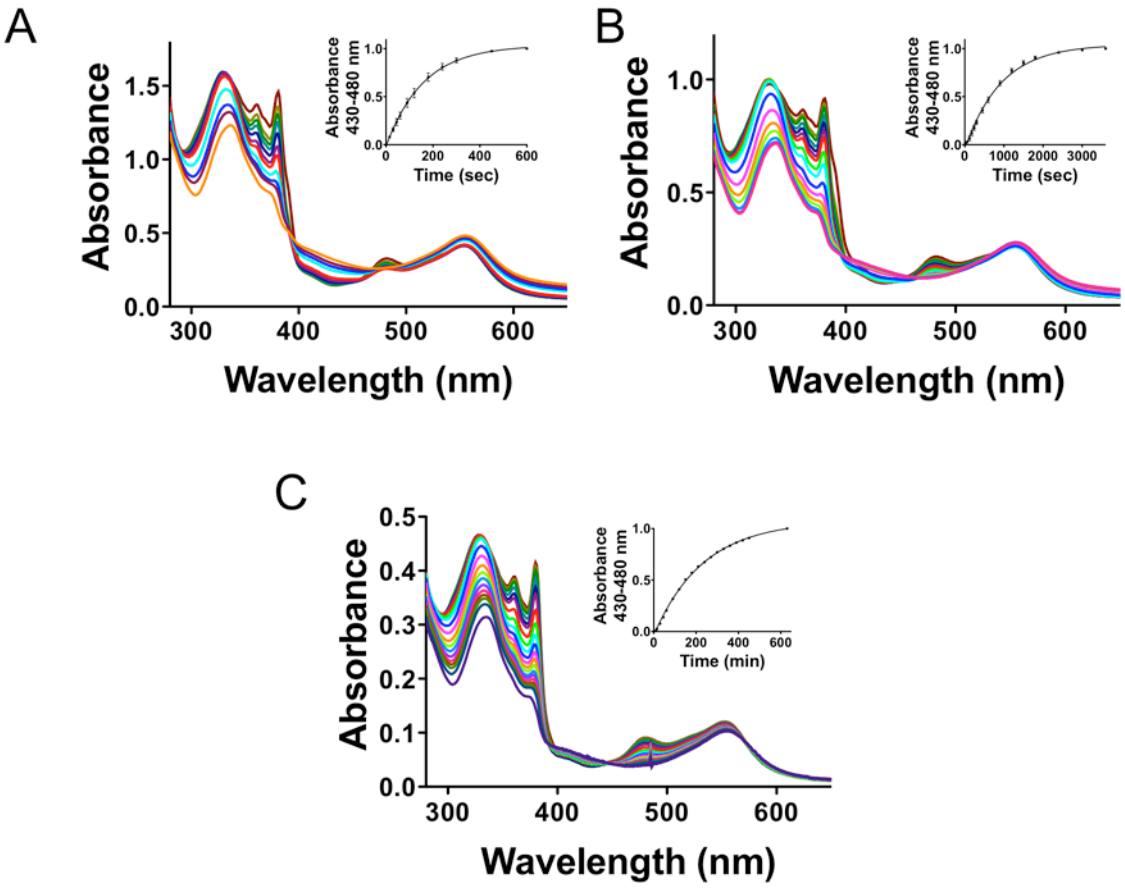

Figure S3. Plots of photoejection kinetics of compound **2** in dH_2O followed by UV/Vis. The kinetic fit is shown in the inset. A) photoejection with green filter; B) photoejection with red filter; C) photoejection with near-IR filter.

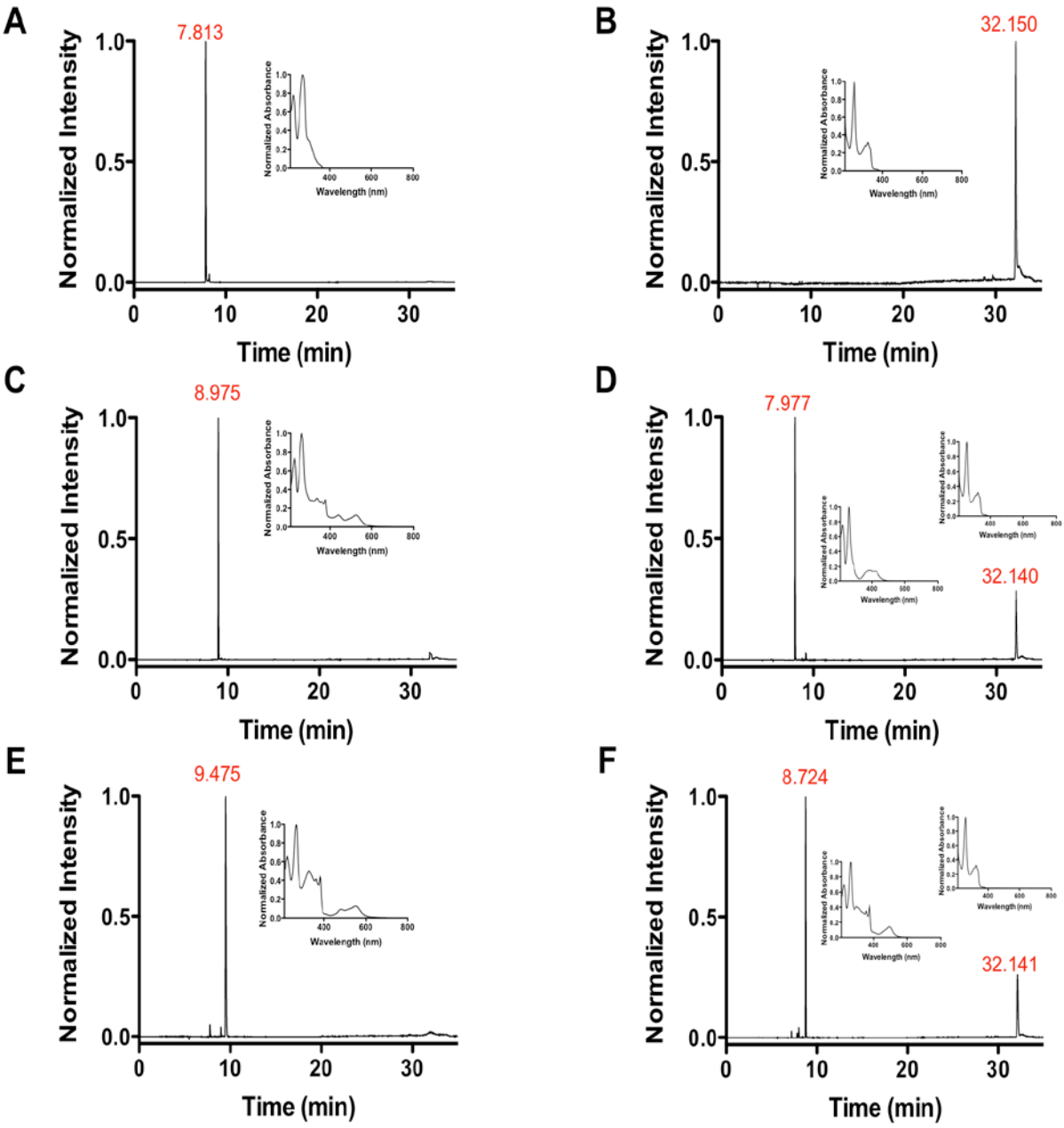

Figure S4. HPLC analysis of compounds **1** and **2** and the ligand ejected after exposure to light. A: 1,10-phenanthroline; B: 2,2'-biquinoline; C: compound **1** before light activation; D: compound **1** after activation; E: compound **2** before light activation; F: compound **2** after activation. Insets show the UV/Vis spectra corresponding to the elution peaks.

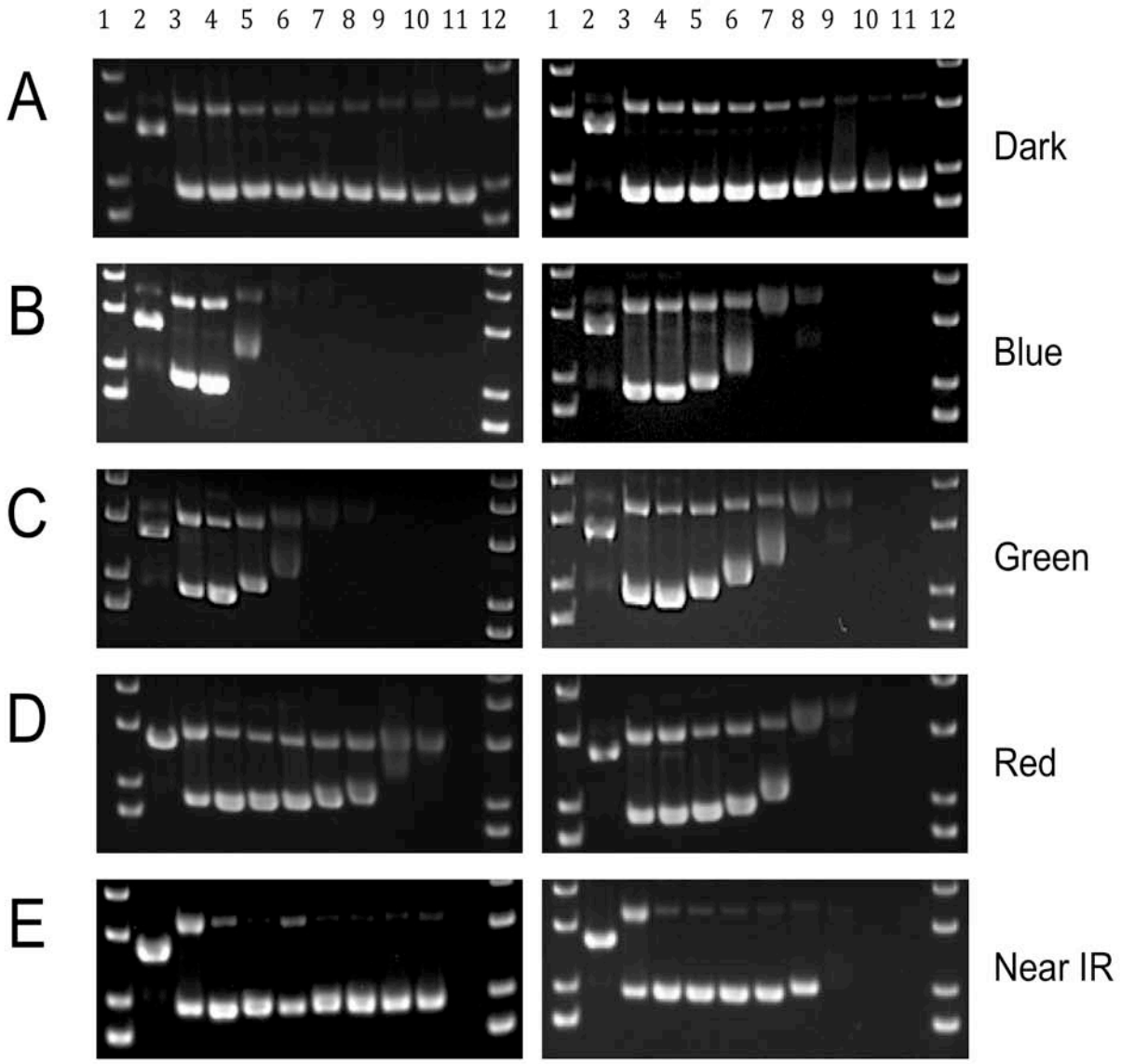

Figure S5. Agarose gel stained with EtBr showing the dose response of **1** (left) and **2** (right) with 40 μg/mL pUC19 plasmid after 1 hour irradiation with various wavelengths of light. A: Dark control, B: Blue (>400 nm), C; Green (>450 nm), D: Red (>600 nm), E: near-IR (>650 nm). Lane 1: DNA Ladder; Lane 2: EcoR1; Lane 3: $Cu(OP)_2$; Lane 4: 0 μM; Lane 5: 15 μM; Lane 6: 30 μM; Lane 7: 60 μM; Lane 8: 125 μM; Lane 9: 250 μM; Lane 10: 500 μM; Lane 11: 1,000 μM; Lane 12: DNA Ladder. EcoR1 and $Cu(OP)_2$ are used as controls for linear and related circular DNA, respectively.

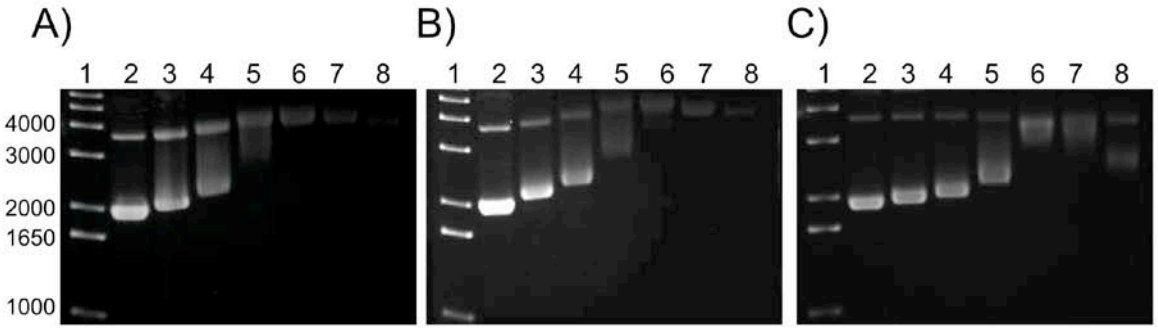

Figure S6. Agarose gel stained with EtBr showing the dose response with 40 μg/ml pUC19 plasmid of A) Compound **1**, 1 hour green light; B) $Ru(phen)_2(H_2O)_2$, 1 hour green light; C) $Ru(phen)_2(H_2O)_2$, dark. The samples were analyzed on a 1 % agarose gel where 1 μg of plasmid was added to each well of the gel. Lane 1: DNA Ladder; Lane 2: 0 μM; Lane 3: 7.5 μM; Lane 4: 15 μM; Lane 5: 31 μM; Lane 6: 62 μM; Lane 7: 125 μM; Lane 8: 250 μM.

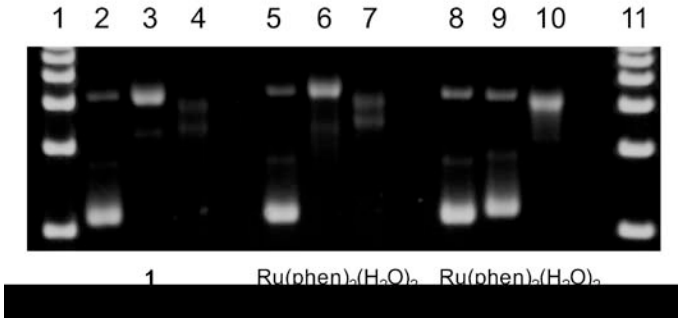

Figure S7. Analysis of pUC19 plasmid previously reacted with compounds and purified. Lane 1 and 11: DNA Ladder. Plasmid was isolated from gel lanes at compound concentrations of 0, 62 and 250 μM from gels in Fig. S6 A), B), and C), above. Gel 6A) Lanes 2, 3 and 4; 6B), lanes 5, 6, and 7; from 6C), lanes 8, 9, and 10. The gel confirms that the samples measured by the Nanodrop contain plasmid DNA. The covalent nature of the adducts and the resulting alteration in the DNA topology are indicated by the retarded migration of the plasmid in the gel, consistent with the original gels from which the samples were purified.

Table S2. Compound **2** selected bond lengths (Å), bond angles (°) and torsion angles (°).

$Ru\text{-}N_{1\text{-}biq(1)}$	2.084(2)	$Ru\text{-}N_{4\text{-}biq(2)}$	2.093(2)
$Ru\text{-}N_{2\text{-}biq(1)}$	2.079(2)	$Ru\text{-}N_{5\text{-}phen}$	2.105(3)
$Ru\text{-}N_{3\text{-}biq(2)}$	2.088(2)	$Ru\text{-}N_{6\text{-}phen}$	2.098(2)
$N_{1\text{-}biq(1)}\text{-}Ru\text{-}N_{2\text{-}biq(1)}$	77.93(10)	$N_{2\text{-}biq(1)}\text{-}Ru\text{-}N_{3\text{-}biq(2)}$	97.14(10)
$N_{1\text{-}biq(1)}\text{-}Ru\text{-}N_{3\text{-}biq(2)}$	104.29(9)	$N_{2\text{-}biq(1)}\text{-}Ru\text{-}N_{4\text{-}biq(2)}$	104.89(10)
$N_{1\text{-}biq(1)}\text{-}Ru\text{-}N_{4\text{-}biq(2)}$	176.23(9)	$N_{2\text{-}biq(1)}\text{-}Ru\text{-}N_{5\text{-}phen}$	169.52(10)
$N_{1\text{-}biq(1)}\text{-}Ru\text{-}N_{5\text{-}phen}$	96.67(9)	$N_{2\text{-}biq(1)}\text{-}Ru\text{-}N_{6\text{-}phen}$	91.42(10)
$N_{1\text{-}biq(1)}\text{-}Ru\text{-}N_{6\text{-}phen}$	82.28(9)	$N_{4\text{-}biq(2)}\text{-}Ru\text{-}N_{5\text{-}phen}$	80.14(9)
$N_{3\text{-}biq(2)}\text{-}Ru\text{-}N_{4\text{-}biq(2)}$	77.98(10)	$N_{4\text{-}biq(2)}\text{-}Ru\text{-}N_{6\text{-}phen}$	95.08(10)
$N_{3\text{-}biq(2)}\text{-}Ru\text{-}N_{5\text{-}phen}$	92.89(9)	$N_{5\text{-}phen}\text{-}Ru\text{-}N_{6\text{-}phen}$	78.87(10)
$N_{3\text{-}biq(2)}\text{-}Ru\text{-}N_{6\text{-}phen}$	170.12(10)		
$N_{1\text{-}biq(1)}\text{-}Ru\text{-}N_{2\text{-}biq(1)}\text{-}C_{10\text{-}biq(1)}$	-20.41(19)	$N_{3\text{-}biq(2)}\text{-}Ru\text{-}N_{4\text{-}biq(2)}\text{-}C_{28\text{-}biq(2)}$	26.1(2)
$N_{2\text{-}biq(1)}\text{-}Ru\text{-}N_{1\text{-}biq(1)}\text{-}C_{9\text{-}biq(1)}$	22.08(19)	$N_{4\text{-}biq(2)}\text{-}Ru\text{-}N_{3\text{-}biq(2)}\text{-}C_{27\text{-}biq(2)}$	-19.5(2)
$N_{1\text{-}biq(1)}\text{-}C_{9\text{-}biq(1)}\text{-}C_{10\text{-}biq(1)}\text{-}N_{2\text{-}biq(1)}$	2.7(4)	$N_{3\text{-}biq(2)}\text{-}C_{27\text{-}biq(2)}\text{-}C_{28\text{-}biq(2)}\text{-}N_{4\text{-}biq(2)}$	12.1(4)
$Ru\text{-}N_{1\text{-}bq(1)}\text{-}C_{9\text{-}biq(1)}\text{-}C_{10\text{-}biq(1)}$	-20.1(3)	$Ru\text{-}N_{3\text{-}biq(2)}\text{-}C_{27\text{-}biq(2)}\text{-}C_{28\text{-}biq(2)}$	10.6(3)
$Ru\text{-}N_{2\text{-}biq(1)}\text{-}C_{10\text{-}biq(1)}\text{-}C_{9\text{-}biq(1)}$	16.1(3)	$Ru\text{-}N_{4\text{-}biq(2)}\text{-}C_{28\text{-}biq(2)}\text{-}C_{27\text{-}biq(2)}$	-28.3(3)
$Ru\text{-}N_{1\text{-}biq(1)}\text{-}C_{1\text{-}biq(1)}\text{-}C_{2\text{-}biq(1)}$	29.6(4)	$Ru\text{-}N_{3\text{-}biq(2)}\text{-}C_{19\text{-}biq(2)}\text{-}C_{20\text{-}biq(2)}$	-11.1(4)
$Ru\text{-}N_{2\text{-}biq(1)}\text{-}C_{18\text{-}biq(1)}\text{-}C_{17\text{-}biq(1)}$	-20.7(4)	$Ru\text{-}N_{4\text{-}biq(2)}\text{-}C_{36\text{-}biq(2)}\text{-}C_{35\text{-}biq(2)}$	36.5(4)
$C_{17\text{-}biq(1)}\text{-}C_{18\text{-}biq(1)}\text{-}C_{1\text{-}biq(1)}\text{-}C_{2\text{-}biq(1)}$	4.48	$C_{35\text{-}biq(2)}\text{-}C_{36\text{-}biq(2)}\text{-}C_{19\text{-}biq(2)}\text{-}C_{20\text{-}biq(2)}$	14.65
$N_{5\text{-}phen}\text{-}Ru\text{-}N_{6\text{-}phen}\text{-}C_{42\text{-}phen}$	-1.5(2)	$Ru\text{-}N_{5\text{-}phen}\text{-}C_{41\text{-}phen}\text{-}C_{42\text{-}phen}$	-1.7(3)
$N_{6\text{-}phen}\text{-}Ru\text{-}N_{5\text{-}phen}\text{-}C_{41\text{-}phen}$	1.7(2)	$Ru\text{-}N_{6\text{-}phen}\text{-}C_{42\text{-}phen}\text{-}C_{41\text{-}phen}$	1.1(3)
$N_{5\text{-}phen}\text{-}C_{41\text{-}phen}\text{-}C_{42\text{-}phen}\text{-}N_{6\text{-}phen}$	0.4(4)		

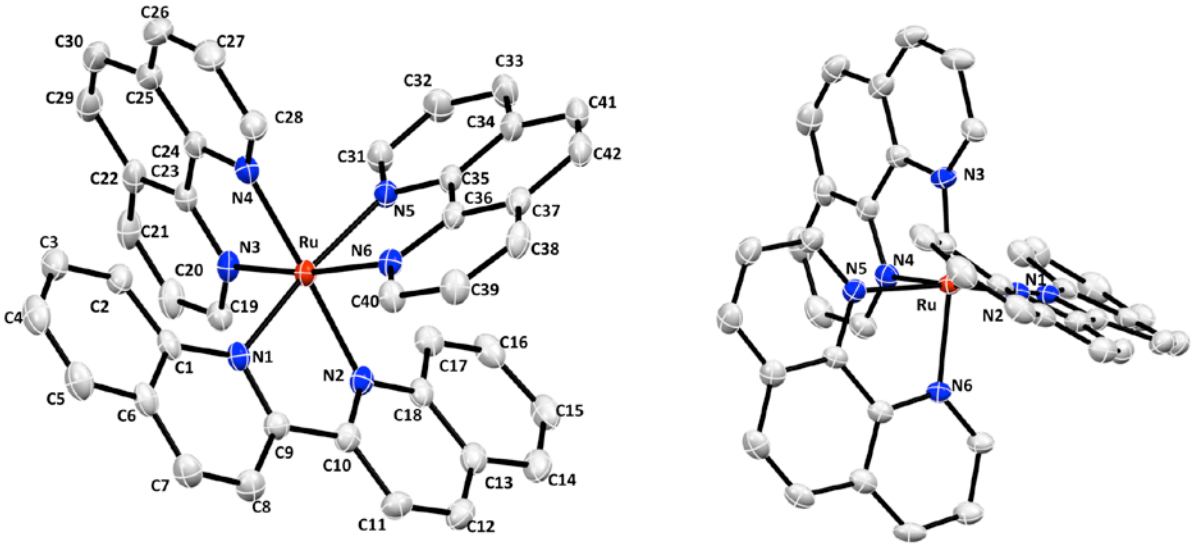

Figure S8. Ellipsoid plot of the cationic view of compound **1**. Ellipsoids are drawn at the 50% probability level, and hydrogen atoms are omitted for clarity. **Left view:** shows labeling of each atom. **Right view:** shows the 20^{o} bend from horizontal of the biquinoline ligand. Note: crystal structure contained two independent cations with only one is shown in this figure.

Table S3. Compound **1** selected bond lengths (Å), bond angles (°) and torsion angles (°).

$Ru-N_{1\text{-}biq}$	2.112(3)	$Ru-N_{4\text{-}phen(1)}$	2.056(3)
$Ru-N_{2\text{-}biq}$	2.095(3)	$Ru-N_{5\text{-}phen(2)}$	2.091(3)
$Ru-N_{3\text{-}phen(1)}$	2.063(3)	$Ru-N_{6\text{-}phen(2)}$	2.091(3)
$N_{1\text{-}biq}-Ru-N_{2\text{-}biq}$	77.62(12)	$N_{2\text{-}biq}-Ru-N_{3\text{-}phen(1)}$	99.15(12)
$N_{1\text{-}biq}-Ru-N_{3\text{-}phen(1)}$	96.15(12)	$N_{2\text{-}biq}-Ru-N_{4\text{-}phen(1)}$	177.93(12)
$N_{1\text{-}biq}-Ru-N_{4\text{-}phen(1)}$	100.41(12)	$N_{2\text{-}biq}-Ru-N_{5\text{-}phen(2)}$	99.29(12)
$N_{1\text{-}biq}-Ru-N_{5\text{-}phen(2)}$	171.15(12)	$N_{2\text{-}biq}-Ru-N_{6\text{-}phen(2)}$	85.65(11)
$N_{1\text{-}biq}-Ru-N_{6\text{-}phen(2)}$	92.22(11)	$N_{4\text{-}phen(1)}-Ru-N_{5\text{-}phen(2)}$	82.75(12)
$N_{3\text{-}phen(1)}-Ru-N_{4\text{-}phen(1)}$	80.35(12)	$N_{4\text{-}phen(1)}-Ru-N_{6\text{-}phen(2)}$	95.11(12)
$N_{3\text{-}phen(1)}-Ru-N_{5\text{-}phen(2)}$	92.52(12)	$N_{5\text{-}phen(2)}-Ru-N_{6\text{-}phen(2)}$	79.23(12)
$N_{3\text{-}phen(1)}-Ru-N_{6\text{-}phen(2)}$	171.08(12)		
$N_{3\text{-}phen(1)}-Ru-N_{4\text{-}phen(1)}-C_{24\text{-}phen(1)}$	-6.2(2)	$N_{1\text{-}biq}-Ru-N_{2\text{-}biq}-C_{10\text{-}biq}$	-20.7(4)
$N_{4\text{-}phen(1)}-Ru-N_{3\text{-}phen(1)}-C_{23\text{-}phen(1)}$	6.3(2)	$N_{2\text{-}biq}-Ru-N_{1\text{-}biq}-C_{9\text{-}biq}$	17.6(2)
$N_{4\text{-}phen(1)}-C_{24\text{-}phen(1)}-C_{2\text{-}phen(1)3}-N_{3\text{-}phen(1)}$	0.2(5)	$N_{1\text{-}biq}-C_{9\text{-}biq}-C_{10\text{-}biq}-N_{2\text{-}biq}$	-5.6(5)
$Ru-N_{3\text{-}phen(1)}-C_{23\text{-}phen(1)}-C_{24\text{-}phen(1)}$	-5.5(4)	$Ru-N_{1\text{-}biq}-C_{9\text{-}biq}-C_{10\text{-}biq}$	-12.3(4)
$Ru-N_{4\text{-}phen(1)}-C_{24\text{-}phen(1)}-C_{23\text{-}phen(1)}$	5.2(4)	$Ru-N_{2\text{-}biq}-C_{10\text{-}biq}-C_{9\text{-}biq}$	20.8(4)
		$Ru-N_{1\text{-}biq}-C_{1\text{-}biq}-C_{2\text{-}biq}$	21.1(5)
$N_{5\text{-}phen(2)}-Ru-N_{6\text{-}phen(2)}-C_{36\text{-}phen(2)}$	2.6(2)	$Ru-N_{2\text{-}biq}-C_{18\text{-}biq}-C_{17\text{-}biq}$	-25.9(5)
$N_{6\text{-}phen(2)}-Ru-N_{5\text{-}phen(2)}-C_{35\text{-}phen(2)}$	2.5(2)	$C_{17\text{-}biq}-C_{18\text{-}biq}-C_{1\text{-}biq}-C_{2\text{-}biq}$	-4.40
$N_{5\text{-}phen(2)}-C_{35\text{-}phen(2)}-C_{36\text{-}phen(2)}-N_{6\text{-}phen(2)}$	-0.4(5)		
$Ru-N_{5\text{-}phen(2)}-C_{35\text{-}phen(2)}-C_{36\text{-}phen(2)}$	-1.9(4)		
$Ru-N_{6\text{-}phen(2)}-C_{36\text{-}phen(2)}-C_{35\text{-}phen(2)}$	2.5(4)		

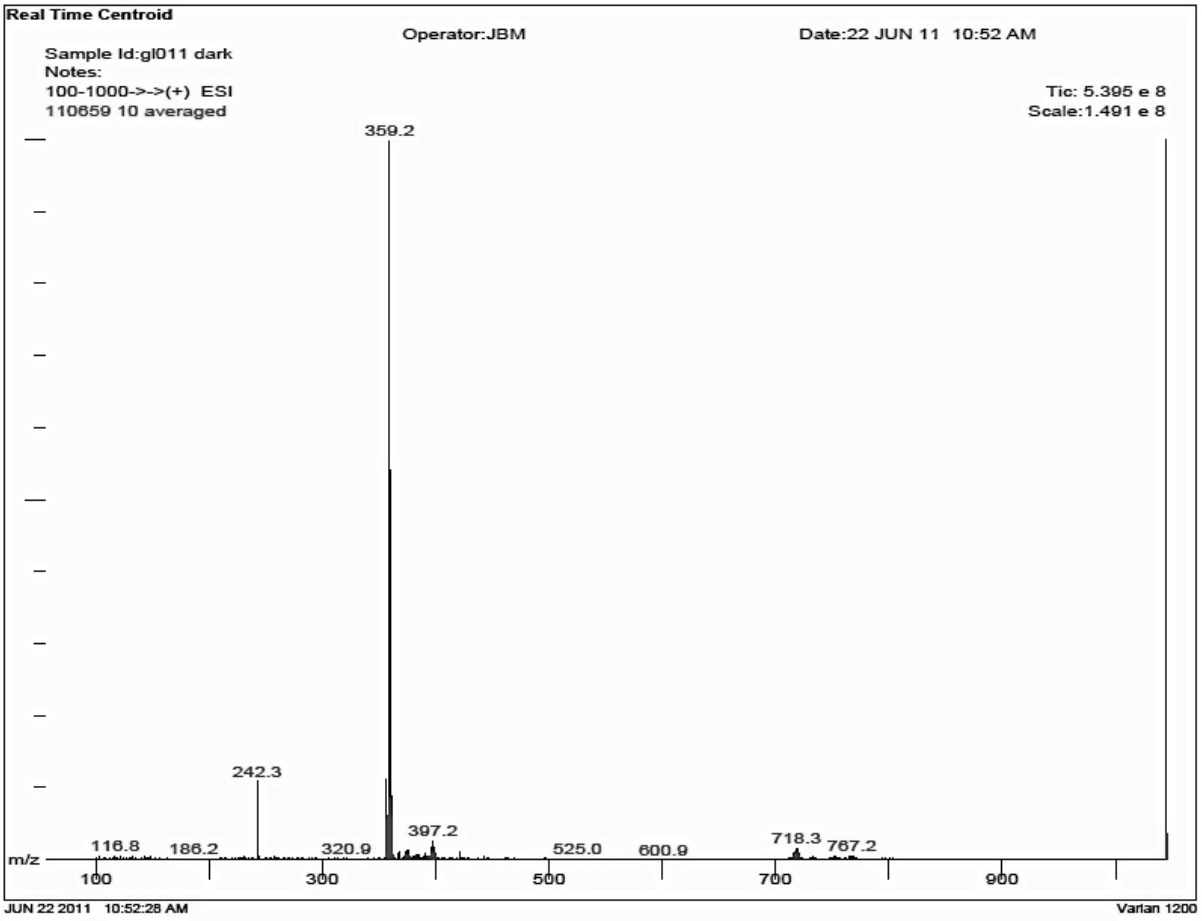

Figure S9. ESI MS of Compound **1**. Peak at m/z 242.3 is tetrabutylammonium. ESI MS calculated for $C_{42}H_{28}N_6Ru$ $[M]^+$ 718.14, $[M]^{2+}$ 359.07; found 718.3 $[M]^+$, 359.2 $[M]^{2+}$.

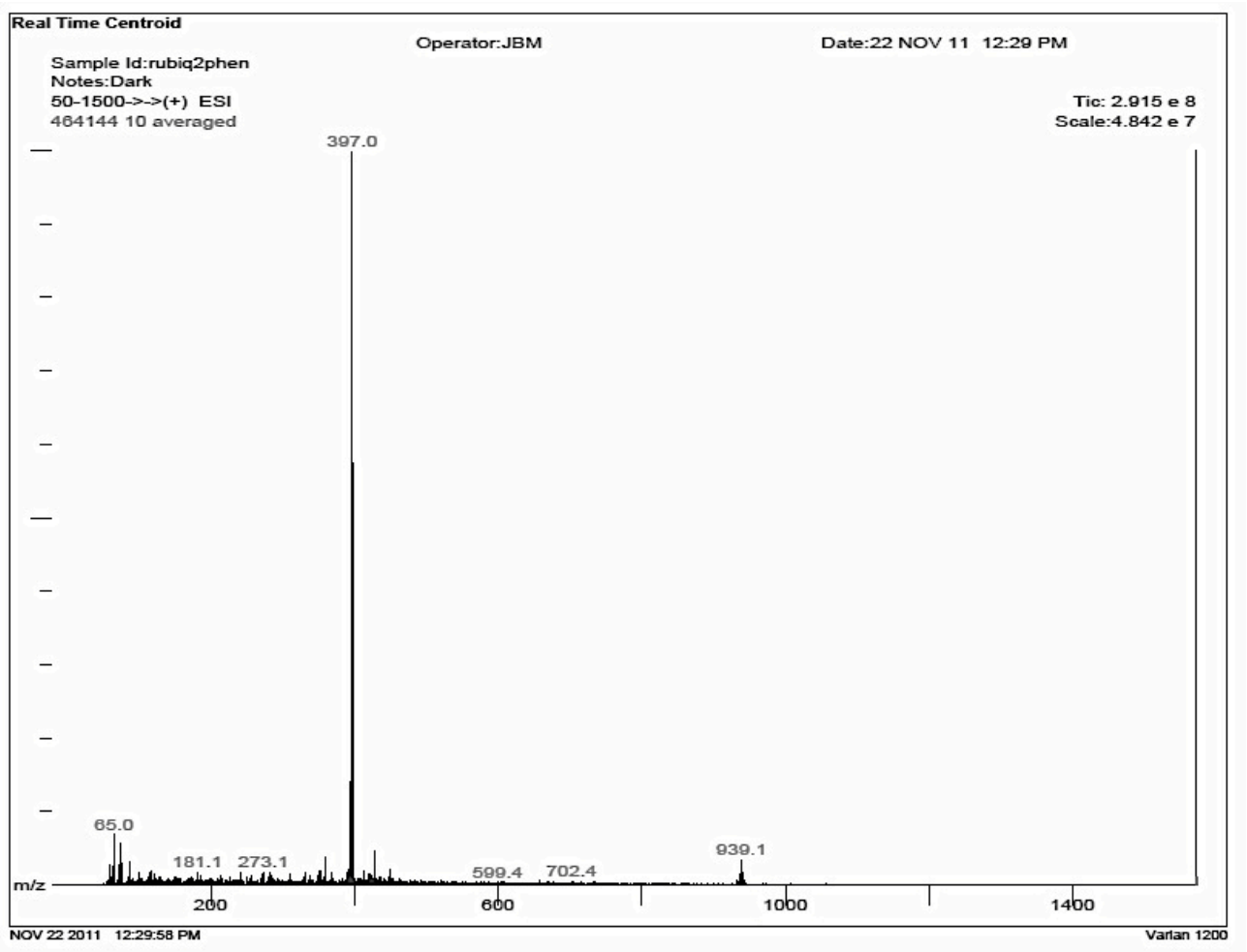

Figure S10. ESI MS of Compound **2**. ESI MS calculated for $C_{48}H_{32}N_6Ru$ $[M]^+PF_6^-$ 939.14, $[M]^{2+}$ 397.09; found 939.1 $[M]^+$ PF_6^-, 397.0 $[M]^{2+}$.

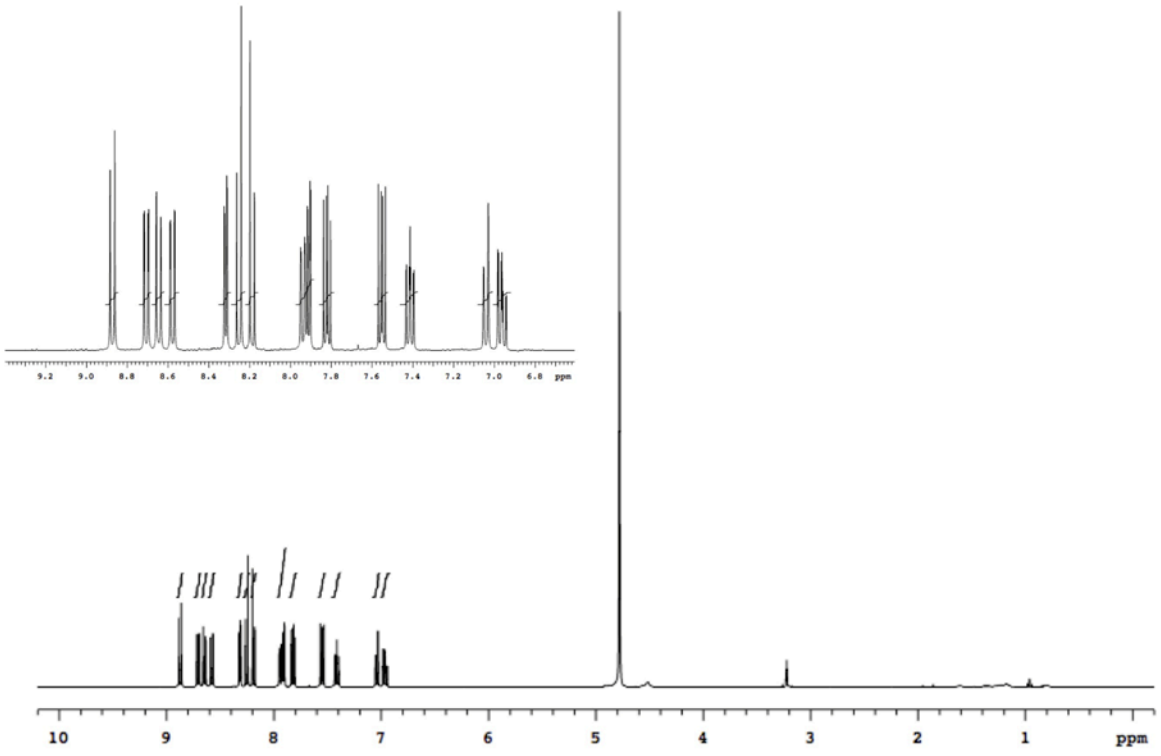

Figure S11. ^{1}H NMR of Compound **1** in CD_3OD**.**

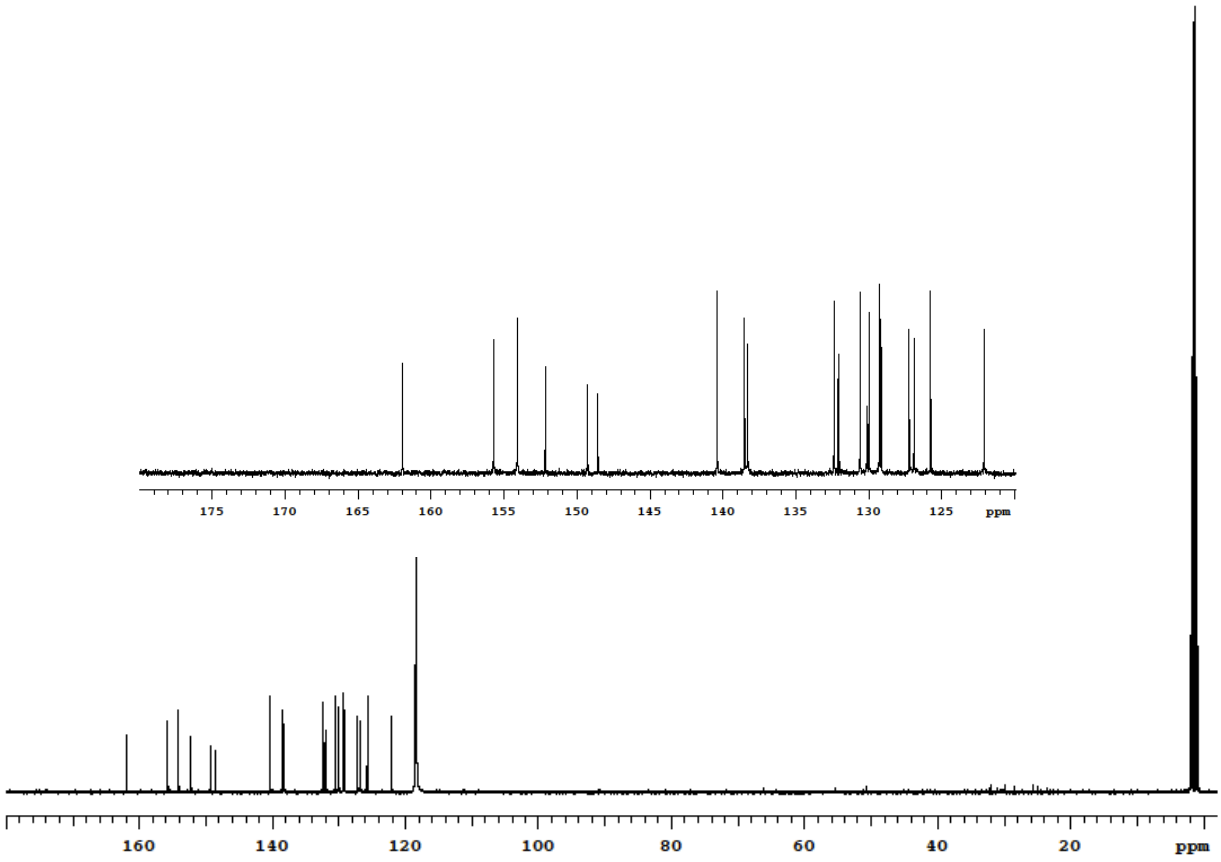

Figure S12. ^{13}C NMR of Compound **1** in CD_3CN**.** Peaks at 1.32 ppm and 118 ppm are residual solvent peaks.

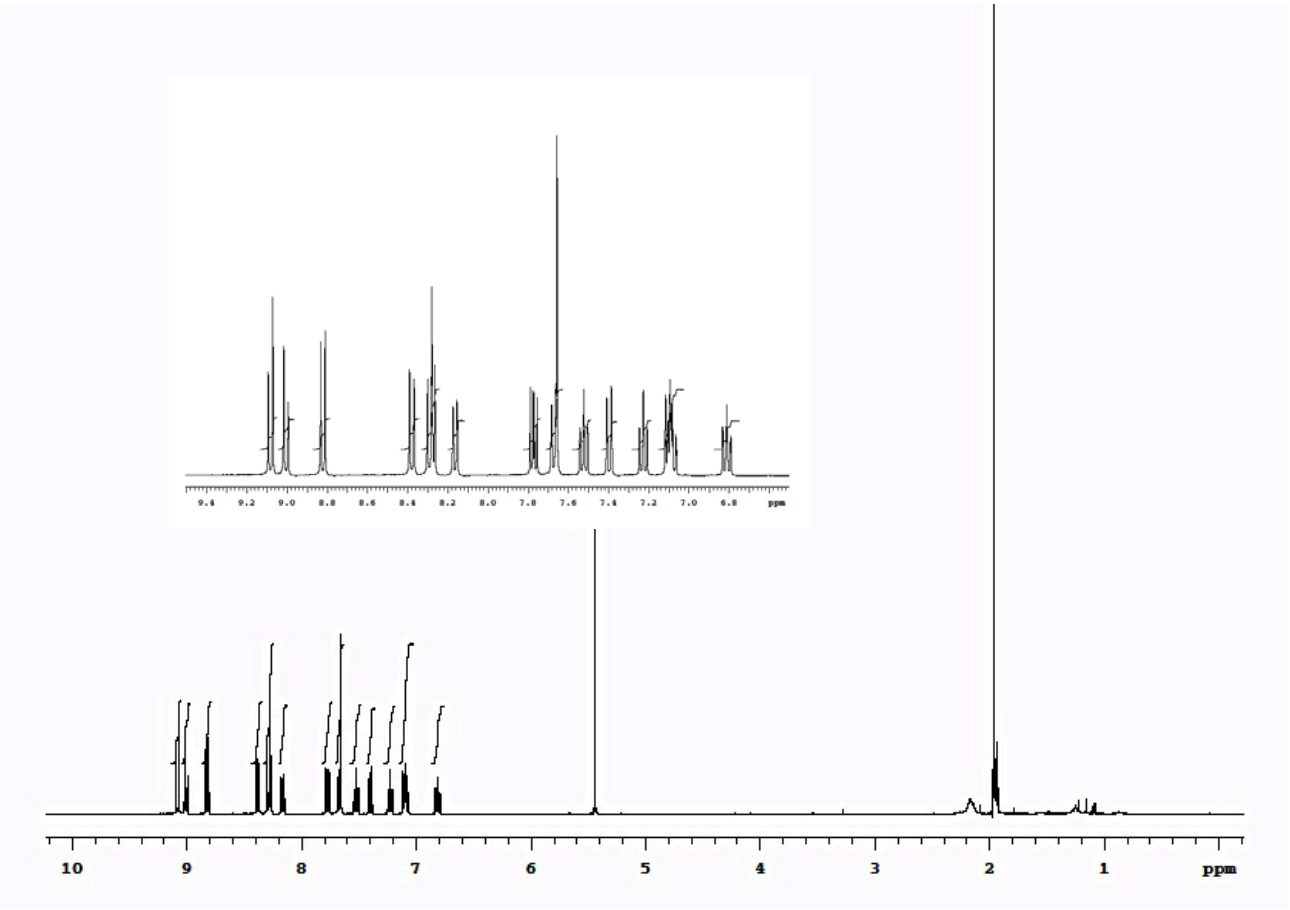

Figure S13. ^{1}H NMR of Compound **2** in CD_3CN**.** The peak at 5.45 ppm is from methylene chloride.

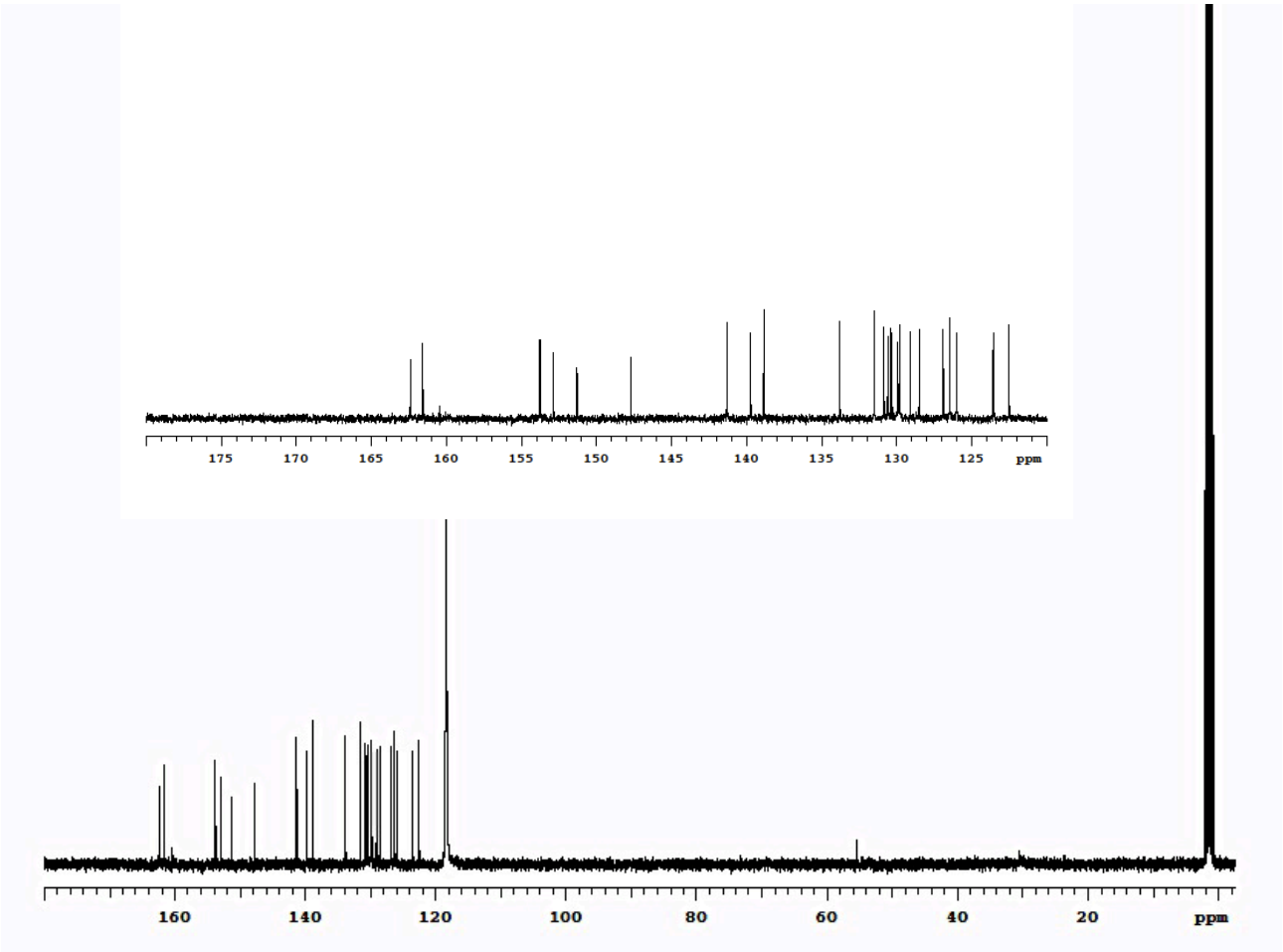

Figure S14. ^{13}C NMR of Compound **2** in CD_3CN**.** Peaks at 1.32 ppm and 118 ppm are residual solvent peaks.

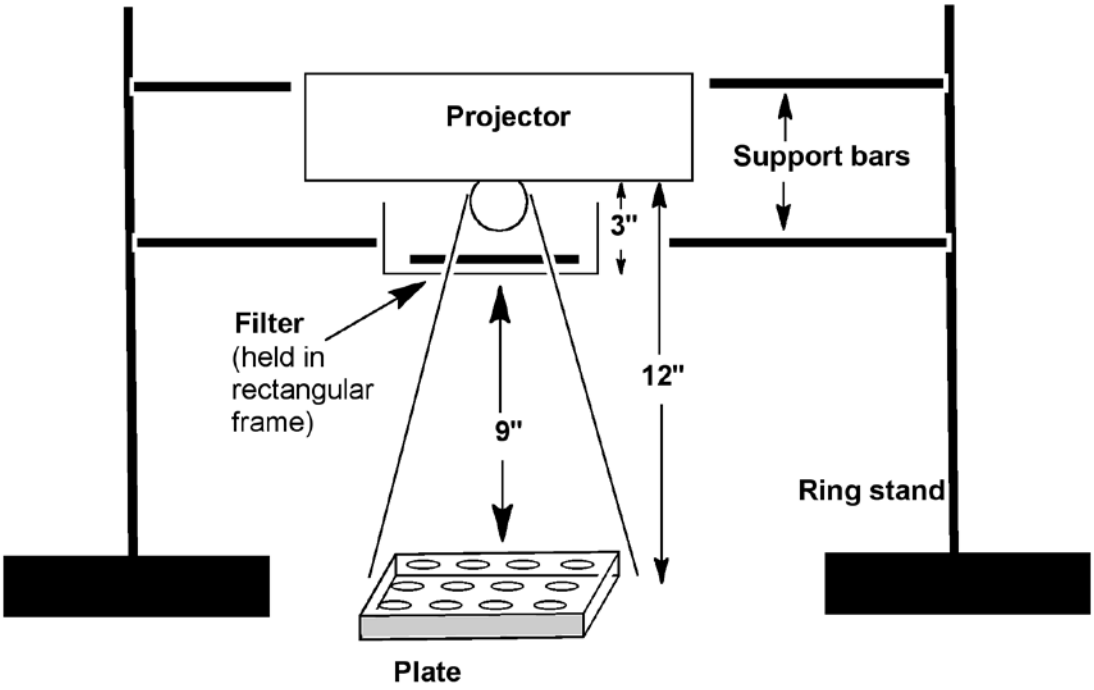

Figure S15. Projector set-up for light activation experiments. The projector and a rectangular frame holding the filter are supported by clamps attached to ring stands. The distance between the projector lens and the plate is 12".

6. References:

1. Keyes, T. E.; Vos, J. G.; Kolnaar, J. A.; Haasnoot, J. G.; Reedijk, J.; Hage, R., *Inorg. Chim. Acta* **1996,** *245* (2), 237-242.
2. Taher, D.; Thibault, M. E.; Di Mondo, D.; Jennings, M.; Schlaf, M., *Chemistry* **2009,** *15* (39), 10132-43.
3. Parkin, S.; Hope H. *J. Appl. Cryst*. **1998**, *31*, (6), 945-953.
4. APEX2 "Programs for data collection and data reduction" **2004**, Bruker-Nonius, Madison WI. USA.
5. Sheldrick, G.M. SADABS & TWINABS. **2008**, University of Goettingen, Germany.
6. Parkin, S.; Moezzi, B.; Hope, H. *J. Appl. Cryst*. **1995**, *28*, (1), 53-56.
7. Sheldrick, G.M. *Acta Cryst*. **2008**, *A64*, (1), 112-122.
8. Parkin, S. *Acta Cryst*. **2000**, *A56*, (2), 157-162.
9. International Tables for Crystallography, Vol C: Mathematical, Physical and Chemical Tables. A.J.C. Wilson, Ed., **1992**. Kluwer Academic Publishers, Holland.
10. Otwinowski Z.; Minor W. "Processing of x-ray diffraction data collected in oscillation mode" *Methods in Enzymology,* **1997** Volume 276: Macromolecular Crystallography part A, pp307-326 C.W. Carter, Jr. & R.M. Swet, Eds., Academic Press.